A Facilely Synthesized Tourmaline-Biochar Composite For Enhanced Removal of Cr (VI) From Aqueous Solution

Qi Lu (luqi@cugb.edu.cn)
China University of Geosciences Beijing https://orcid.org/0000-0002-9100-9523
Siyi Huang
China University of Geosciences Beijing
Xiaorui Ma
China University of Geosciences Beijing

Research Article

Keywords: Tourmaline, biochar, composite, adsorption, Cr (), removal mechanism

Posted Date: August 10th, 2021

DOI: https://doi.org/10.21203/rs.3.rs-728034/v1

Abstract

A tourmaline-biochar composite (TMBC) was facilely synthesized to effectively remove Cr (Ⅵ) from aqueous solution. The effects of different ratio (TM: BC) and pyrolysis temperature on TMBC adsorption performance were compared for optimal condition of TMBC preparation. The TMBC samples were characterized by X-ray diffraction (XRD), Fourier transform infrared (FTIR) and scanning electron microscope-energy dispersive spectrometer (SEM-EDS). The kinetics and thermodynamics were analyzed to investigate the sorption mechanism for removal of Cr (VI). The results showed that the proper pyrolysis temperature was 650℃, and the ratio of TM and BC was 1:3. SEM results showed that there are many pores in the biochar structure, which is helpful for tourmaline dispersion. The adsorption kinetics was fitted well by the pseudo-second-order model, indicating the sorption is related to chemical absorption. Freundlich adsorption isotherms suggested monolayer adsorption between Cr (Ⅵ) and TMBC, and the maximum adsorption capacity of TMBC for Cr (Ⅵ) was 53.10 mg/g at initial pH 4.0, which is more than twice higher than pristine TM (17.85 mg/g). Such adsorption mechanisms included water automatically polarized, ion exchange and electrode adsorption, among which the automatic polarization of water caused by tourmaline was the unique adsorption property of TMBC. So TMBC composite can be used as an economic adsorbent in the remediation of heavy metal pollution in water.

Highlights

- Tourmaline-biochar composite TMBC was facilely synthesized for high adsorption of Cr (VI).
- Tourmaline is evenly distributed on the surface of biochar to promote Cr (VI) adsorption.
- Cr (VI) adsorption on TMBC was related to monolayer and chemical sorption.
- The unique absorption mechanism of TMBC is mainly self-polarization of tourmaline surface.
- TMBC exhibits excellent performance on Cr (VI) removal in acidic wastewater.

Introduction

Heavy metal pollution in the water is one of the important environmental issues. Typically, Cr (Ⅵ) is a concerned contaminant due to its high solubility and toxicity. Cr (Ⅵ) can enter human body along with food and water, resulting in mutagenic diseases, such as kidney injury, chronic ulcers, and lung cancer (Zheng et al. 2019). The World Health Organization recommended guideline value for total Cr in drinking water is 0.05 mg/L (Fang et al. 2020). Therefore, highly effective removal of Cr (Ⅵ) from polluted water is necessary for the environmental remediation. Up to now, the methods of ion exchange, solvent extraction, precipitation, membrane technology, electrochemical treatment and adsorption, have been used to remove heavy metals from water (Rahman et al. 2020; Pavithra et al. 2017; Jiang et al. 2015; Yao et al. 2012 Liu et al. 2011). Specifically, adsorption is attractive for its easy operation, high efficiency, low cost and environmental friendliness. Many economic adsorbents such as bentonite (Yang et al. 2010), kaolinite (Mostafa et al. 2019), carbon (Lalhmunsiama et al. 2013) and biochar (Matthew et al. 2017; Han

et al. 2016; Mohan et al. 2014; Ahmad et al. 2014; Sobhanardakani et al. 2013), were developed to absorb and remove heave metals from contaminated water.

Tourmaline is a natural mineral with unique physical and chemical properties, such as producing electrostatic field and releasing rare trace elements. The adsorption of heavy metals by tourmaline is due to its polarization mechanism, which is a unique adsorption mechanism (Yan et al. 2021; Nakamura et al. 1992). The most important electrical property of tourmaline is its spontaneous and permanent poles, which can produce electric dipoles, especially in small particles with a diameter of a few microns or smaller (Xia et al. 2006). Tourmaline belongs to trigonal crystal system, and the general formula is $XY_3Z_6Si_6O_{18}$ (BO_3) W_4. X site is usually occupied by various cations, such as Ca, Na, K, or vacancy, Y position can be occupied by Fe, Mg, Mn, Al, Li, and Ti, and Z site is usually occupied by Al (also replaced by Fe^{2+}, Fe^{3+}, Ti, Mg, Cr and V^{3+}). W site is occupied by OH, but can also be replaced by F and O. Therefore, there are various cation and anion sites in tourmaline structure. In order to obtain higher removal efficiency, tourmaline is made into smaller particles to enhance its automatic polarization ability (Ruan et al. 2003).

Additionally, modifying tourmaline can be used to make composites with TiO_2 (Liang et al. 2010), carbon (Bi et al. 2021), porous ceramisite (Xu et al. 2016), montmorillonite (Chen et al. 2020) and rare-earth elements (Zhu et al. 2010). for better performance, such as tensile strength, antibacterial ability and surface area (Lehmann et al. 2006). To enhance the adsorption capacity of tourmaline towards heavy metals Cr (VI), the modification by biochar was potentially feasible in that biochar has large surface energy, rich pore structure and functional groups (Le et al. 2019; Dinesh et al. 2014). The combining of tourmaline and biochar can reduce the agglomeration of tourmaline particles and biochar structure for remarkable increase of the sorption capacity.

The purpose of this study was to investigate the feasible synthesis approach to a new composite derived from tourmaline and biochar (TMBC) and assess the effectiveness of removing Cr (□) from aqueous solution. In particular, the synthesis was focused on optimal condition for the different ratio of tourmaline/biochar and composite pyrolysis temperature. The adsorption mechanism was elucidated by the kinetics/isotherms experiments and the characterization of composite. The results from this study could provide valuable modified tourmaline with biochar as an economic efficient adsorbent for wastewater treatment.

Materials And Methods

2.1 Materials

Tourmaline with average particle size of 1.3μm was purchased from Hualang Mineral Products Processing Plant, Shijiazhuang, Hebei Province, China. The biochar feedstock Chestnut shells were collected from the farmlands of Fengnan county, Hebei province, China, and thoroughly washed using deionized water (18.3MΩ·cm) and air-dried at room temperature (25 ± 0.5℃), and ground into small

particles. Potassium dichromate ($K_2Cr_2O_7$), sulfuric acid (H_2SO_4), phosphoric acid (H_3PO_4) and acetone were purchased from Sinopharm Chemical Reagent Co., Beijing, China. Cr (VI) stock solution was prepared by dissolving potassium dichromate in deionized water. All the chemicals in this study were analytical grade, used without further purification. All the solution in the experiments was prepared using deionized water.

2.2 Preparation of TMBC

Tourmaline (TM, 20g) with different ratio of pretreated biomass (BC, 6.67, 10, 20, 40, 60g) were mixed in a beaker, and all materials were mixed in dry state, then deionized water was added to the beaker and stirred for 24 h. Then, the mixed material was dried in oven (DZ-2BCIV, Tianjing, China) until it reached to a constant weigh. Finally, the dried mixture was placed in a muffle furnace (SX2-4-10, Tianjin Central Experimental Electric Furnace Co., Tianjin, China). The furnace was heated to 450°C, 550 ℃ and 650 ℃ at a rate of 5°C/min and the peak temperature was then maintained for 2 h. After naturally cooling, the obtained composite (TMBC) pyrolyzed at 450°C, 550 ℃ and 650 ℃ denoted as TMBC-450, TMBC-550 and TMBC-650, respectively. The different proportions of TM: BC were prepared for composite (TMBC) from 25–75% (w/w) corresponding to the TM: BC (w: w) ratio of 1:3, 2:3, 1:1, 3:2, and 3:1, respectively, and the composite was synthesized under the same condition.

2.3 Characterization of TMBC

The crystal structures of the samples were examined by X-ray Diffraction (XRD) performed on Smart-Lab (Japan) using Cu Ka radiation in the range of 10˚-90˚(2θ). Scanning electron microscopy (SEM) was applied to characterize the morphology and the equipped energy dispersive spectrometer (EDS) was to analyze the chemical composition. The surface functional groups were identified with Fourier transform infrared spectrometer (FTIR, Tensor 27, German).

2.4 Adsorption of Cr (VI) by TMBC

Cr (Ⅵ) solution with the concentrations (50–550 mg/L) was prepared by dissolving certain amount of K_2CrO_7 (200 mg/L) in deionized water. The desired pH of initial solution (4–10) was adjusted using 0.1 M HCl or NaOH and the pH value was monitored by a pH meter (PB-10, Sartorius, Sartorius, Goettingen, Germany).

For adsorption kinetics, Cr (Ⅵ) at an initial concentration of 50 $mg{\cdot}L^{-1}$ was mixed with 80 mg composites in 50 mL centrifuge tubes, at a solid-to-liquid ratio of 1:500. All vials were sealed with Teflon screw caps and shaken at 180 $r{\cdot}min^{-1}$ at 25°C. About 5 mL supernatant was withdrawn from each vial after 0, 30, 60, 90, .., ….550min. The supernatants were filtered through 0.22μm polyether sulfone filters, measured at 540 nm on UV-visible spectrophotometry (UV1750, Shimadzu, Kyoto, Japan) by 1,5-diphenylcarbazide method.

Adsorption isotherms experiments were conducted in 10-mL centrifuge tubes by mixing 16 mg of composites with 8 mL of Cr (VI) solution. All vials were shaken at 180 $r{\cdot}min^{-1}$ for 24 h, based on the

equilibrium time established in the prior kinetics experiment. The vials were placed up to solid–liquid separation, and about 5 mL supernatant withdrawn, filtered through a 0.22-μm polyether sulfone filter and measured at 540 nm on UV-visible spectrophotometry. The adsorption capacity (Qe) for Cr(Ⅵ) was calculated from the following Eq. (1):

$$Q_e = \frac{(C_0 - C_e)V}{m} \quad (1)$$

where C_0 (mg/L) and C_e (mg/L) are the concentrations of Cr (Ⅵ) at the initial time and equilibrium liquid phase; V (L) is the volume of the solution; and m (g) is the mass of adsorbent used.

Results And Discussion

3.1 The sorption performance of TMBC

The adsorption performance of TMBC composite (10g) on the removal of Cr (VI) (200mg/L) in potassium dichromate solution (pH = 4) was compared in Fig. 1(a), which showed the adsorption ability of TMBC-450, TMBC-550, TMBC-650 was 34.82, 37.69 and 41.10 mg/g, respectively. TMBC-650 exhibited the highest adsorption performance in that the thermally activated tourmaline has more specific surface area and negatively charged surface, which could enhance the adsorption of heavy metal ions (Li et al. 2015; Wang D et al. 2018). As a consequence, the adsorption of Cr (VI) would increase because of the enhancement of electrostatic repulsion and the strengthening of the polarity of tourmaline (Wang et al. 2019).

The sorption of Cr (VI) on TMBC-650 with different ratio of TM:BC (1:1, 1:2, 1:3, 2:1, 3:1) was compared in Fig. 1(b), showing different adsorption behaviors. When the proportion of TM was 50%, the adsorption efficiency was the lowest with a capacity of 33.43 mg/g. And when it decreased to 25%, the adsorption capacity increased to the highest level (42.86 mg/g). When the proportion of TM increased to 66.6% and 75% (w/w), the adsorption capacity decreased to 35.96 mg/g and 34.86 mg/g, respectively. The composite would produce agglomerate and disperse unevenly with increasing proportion of TM, so the adsorption efficiency of Cr (VI) on the composites decreased with the increasing of TM. However, TM in the composite would not get enough dispersed when TM increased too much. TM might be agglomerated and waken its ability of polarizes spontaneously. Besides, the composite might disperse easily and not bind tightly when BC in low proportion. Thus, the composite TMBC-650 with 25% of TM performed the optimal adsorption performance and it was employed for the following characterization and experiments.

3.2 Characterization of TMBC

Scanning electron microscopy (SEM) images of TM, BC and TMBC-650 were shown in Fig. 2. The surface of TM was smooth, while the BC showed loose and porous. TMBC-650 showed many clusters and the surface was rough and multilayer, which was effective for TMBC to absorb heavy metals.

The surface chemical analysis of TMBC was studied by energy dispersive spectrometer (EDS) as shown in Fig. 2. The main elements were C, O, Si, Fe, Al and Ca and the oxygen accounted for 26.88% of the total

mass, which was about six times of the silicon content. It concluded that TMBC might contain a large amount of oxygen-containing functional groups and oxides, such as hydroxyl groups, carboxyl groups, aluminum oxide and ferrous oxide, which could combine with metal ions in wastewater (Jia et al. 2018).

The crystallographic structures of TM, BC and TMBC were identified by X-ray diffraction (XRD) in Fig. 3. TM has a complex structure, with different peaks at the diffraction angles of 14.35°,17.02°,18.75°, 20.933°, 22.018°, 26.62°, 28.768°, 34.501°, 44.569°, 46.876°, 55.763° and 64.785°, indexing to characteristic peaks of tourmaline (Hawthorne et al. 1999). BC has no obvious diffraction peaks due to amorphous material. TMBC possessed the same diffraction peaks of TM and BC, demonstrating that the sintering process did not damage the crystal structure of the raw material and tourmaline might be uniformly dispersed in biochar.

The FTIR spectra of the samples were recorded in Fig. 4, and TMBC have more absorptions bands than TM and BC between 400cm^{-1}-2000cm^{-1}. The main peak at 945 cm^{-1} and 1047 cm^{-1} were corresponded to Si-O-H stretching vibration and O-Si-O stretching, respectively (Wang F et al. 2018). The bands at 710 cm^{-1} and 780 cm^{-1} were ascribed to the bending stretching of M-O (M = Fe, Mg or Al), indicating that the surface groups were attached on the surface metallic ions, which were likely potential active sites during the adsorption (Yin et al. 2015). The absorption band at 1649 cm^{-1} was ascribed to H-O-H (Barbier et al. 2000).

3.3 Kinetics and isotherms of Cr (VI) adsorption on TMBC

The adsorption kinetics of Cr (VI) g/L) on TMBC (g) in mL water (pH = 4) was carried out and the experimental data were fitted using pseudo-first-order and pseudo-second-order kinetic models in the following Eqs. (2)-(3).

$$Q_t = Q_e (1-e^{-k1t}) \quad (2)$$

$$Q_t = Q_e^2 k_2 t/(1 + Q_e k_2 t) \quad (3)$$

Where Q_t (mg/g) is the adsorption amount at time t (min), k_1, k_2 are the rate constants, corresponding to the first-order adsorption (1/min) and the pseudo-second-order adsorption (g/ (mg· min)), Q_e (mg/g) is the maximum amount of adsorption per unit mass of adsorbent in equilibrium.

As shown in Fig. 5a, the adsorption capacity of TM, BC and TMBC increased rapidly within 200 minutes, and then slowed down to reach the equilibrium within 420 minutes. The maximum adsorption capacity of TMBC was 53.10 mg/g, which was much higher than that of TM and BC. The adsorption process was fast at early time due to many adsorption sites available at the initial stage of adsorption, low mass transfer resistance on the surface of adsorbent and fast adsorption reaction speed. As the surface adsorption sites were gradually filled up, the adsorption was more dependent on the transport of adsorbate from the external sites to the internal sites of the adsorbent, and the adsorption speed was reduced (Yu et al. 2000).

The adsorption kinetics models fitted the experimental data and the parameters were listed in Table 1. It showed that the pseudo-second order is better than the pseudo-first order kinetic model for Cr (VI) adsorption by TM, BC and TMBC. This indicated that the adsorption behavior of Cr (VI) on TMBC was more related to chemical absorption (Cheng et al. 2008). During heat treatment at higher temperature dehydrated hydroxyl groups was incorporated in the crystal lattice, and tourmaline may undergo chemical reaction. Different from Cr (VI)) adsorption on TM and BC, the composite of TMBC mainly depends on the ion exchange sites and specific adsorption sites (Barbier et al. 2000). The adsorption of Cr (VI) on TMBC is mainly due to its special adsorption mechanism and structural characteristics of TM, such as spontaneous polarization, release of negative ions and resolution of metal bonds (Zhang et al. 2011). The results showed that the adsorption capacity of TMBC was greatly improved, and the combined process had a positive effect on the adsorption. SEM results showed that there are many pores in the biochar structure, which is helpful for tourmaline dispersion. Thus, the addition of biochar can reduce the aggregation of tourmaline, which improve the spontaneous polarization of tourmaline. In addition, the increase of specific surface area of micro-size tourmaline can provide many sites for Cr (VI) adsorption. Moreover, high temperature treatment can activate the negative surface charge and specific surface area of tourmaline (Chen et al. 2019), improve the thermal stability of tourmaline, and enhance the adsorption properties of TMBC composites.

Table 1 Model fitting parameters for adsorption kinetics of Cr (VI) by TM, BC and TMBC.

Sample	Pseudo-first-order			Pseudo-second-order		
	Qe (mg/g)	K_1(1/min)	R^2	Qe(mg/g)	K_2(1/min)	R^2
TM	16.38	0.00639	0.746	17.84	0.00373	0.902
BC	18.89	0.00717	0.857	18.35	0.00126	0.924
TMBC	43.58	0.00730	0.988	43.64	0.00718	0.993

Langmuir model Eqs. (4) and Freundlich model Eqs. (5) were used to describe the isothermal adsorption of Cr (VI) on TMBC.

Langmuir isotherm: $Qe = \frac{Q_{max} K_L C_e}{1+K_L C_e}$ (4)

Freundlich isotherm: $Qe = K_F C^{1/n}_e$ (5)

Where Qe (mg/g) is the equilibrium adsorption capacity, Ce (mg/L) is the concentration of adsorption equilibrium, Q_{max} (mg/g) is the maximum sorption capacity, K_L, K_F are the Langmuir constant (L/mg) and Freundlich constant ((mg/g) $(mg/L)^{-n}$), respectively, and 1/n is the adsorption intensity.

The adsorption isotherms of Cr (VI) on TMBC were shown in Fig. 5(b) and the model fitting parameters were listed in Table 2. The Langmuir model was more consistent with the experimental data, and the R^2 value of the former is closer to 1 than that of the Freundlich model. In addition, the adsorption of Cr (VI)

on TMBC surface is monolayer adsorption. The molecular weight distribution was even, and the adsorption energy on the surface was uniform (Awual et al. 2014). Due to the great contribution of ions, this led to the inhomogeneity of surface exchange sites (Zhou et al. 2015). At the same time, the 1/n value in Langmuir isotherm was less than 1, indicating that the adsorption of Cr (VI) by TMBC was a chemical adsorption (Duan et al. 2018). The results showed the maximum adsorption capacity of TMBC for Cr (VI) was 55.10 mg/g.

Table 2 Model fitting parameters for isothermal adsorption of Cr (VI) by TMBC.

Sample	Langmuir model			Freundlich model		
	Qm(mg/g)	K_L (L/mg)	R^2	Q_m(mg/g)	K_L (L/mg)	R^2
TMBC	55.10	0.0064	0.992	44.74	0.0321	0.962

3.4 Effects of solution pH on Cr (VI) adsorption by TMBC

The adsorption of Cr (VI) (200mg/L) on TMBC (24mg) in 50mL water was compared under the effect of different initial pH values from 4.0 to 10.0 as shown in Fig. 6. When the pH increased from 3.0 to 7.0, the removal efficiency of Cr (VI) by TMBC decreased, while increased from pH 7.0 to 10.0. The maximum adsorption was only 19.89 mg/g at pH 7, While the maximum of adsorption was 43.01mg/g at pH 4. In addition, the adsorption efficiency of TMBC for Cr (VI) in acidic condition is better than that in alkaline or neutral condition. Such behavior is attributed to the neutral pH of the solution associated with the polar mechanism of tourmaline (Xia et al. 2006). The results suggested that TMBC is a nice absorption for the removal of Cr (VI) in acidic wastewater.

3.5 Adsorption mechanism

In this study, TMBC composite with strong adsorption capacity for the removal of Cr (VI) was obtained by sintering tourmaline and biochar. The adsorption mechanism of TMBC can be explained by the following factors. Firstly, tourmaline can be polarized automatically in TMBC and produce negative ions as Eqs. (6)-(9) (Li et al. 2016). Meanwhile, the M-O bond (m = Na, Mg or Fe) of metal ions on tourmaline surface is easy to decompose, and then exposed to a large range of aqueous solutions. These ions are easily attracted by polar water molecules, leaving the crystal surface and entering into water phase, which results in many negative potentials on the mineral surface.

$H_2O \rightarrow H^+ + OH^-$ (6)

$OH^- + H_2O \rightarrow OH^- (H_2O)_n$ (7)

$Cr^{6+} + OH^- \rightarrow Cr(OH^-)^{5+}$ (8)

$Cr^{6+} + OH^- (H_2O)_n \rightarrow Cr(OH^-)^{5+} (H_2O)_n$ (9)

$Cr^{6+} + 6Si\text{-}O\text{-}H^{-} \rightarrow 6Si\text{-}O\text{-}Cr + 6H^{+}$ (10)

Secondly, there are a lot of siloxanes and silanol groups on the surface of TMBC as shown in Fig. 4, which can significantly improve the adsorption performance of Cr (VI). Some Si-O bonds can be directly broken and interact with water molecules. So the surface of TMBC can be hydroxylated and Cr (VI) can directly replace the protons as Eqs. (10). On the other hand, the oxygen atoms in the solution can directly complex with Cr (VI) or $Cr^{6+}(H_2O)_n$ to reduce the concentration of Cr (VI) (Wang et al. 2012). As FTIR spectrum of TMBC-Cr in Fig. 7, the absorption peaks of 719cm^{-1} and 783 cm^{-1} represent the spectral vibration of Cr-O, and the absorption peak of 1045 cm^{-1} represents the spectral vibration of Si-O-Cr.

Thirdly, the cation exchange mechanism plays an important role in the removal of heavy metals. The cations such as $Fe^{3+}$and Cu^{2+} on the surface of TMBC can be replaced by Cr (VI), then the concentration of TMBC can be reduced by complex adsorption. Therefore, TMBC can adsorb Cr (VI) by electrostatics and complexation, such as metal bonds on composite surface, hydroxylation and self-polarization.

Conclusion

The composite of tourmaline and biochar (TMBC) were prepared successfully by different pyrolysis temperature and different ratio, which has good adsorption performance for Cr (VI) in aqueous solution. The results show that the optimum condition of the composites polysized at 650℃, with the ratio of 1:3 (TM and BC), which has the highest absorption, reaching 53.10 mg/g. The results of EDS, FTIR and XRD show that TMBC are mainly composed of O, Si, Fe, Al and Ca. The crystal structure of the TMBC composite has abundant siloxane and silanol groups. Batch experiments show that the adsorption of Cr (VI) by TMBC is a monolayer adsorption process. Cr (VI) is mainly bind to the surface of TMBC to form an inner sphere complex, and the maximum adsorption capacity can reach 53.10 mg/g. The absorption mechanism is mainly self-polarization of tourmaline surface, which could provide silanol hybrid groups and promote surface electrostatic adsorption for Cr (VI). Therefore, TMBC can be used as a low-cost and efficient adsorbent to remove Cr (VI) from wastewater, especially in acidic solution. The application of tourmaline as adsorbent in the remediation of heavy metal pollution provides a valuable reference for the removal of metal pollution in water.

Declarations

The authors declare that they have no known competing financial interests or personal relationships that could have appeared to influence the work reported in this paper.

Ethics approval and consent to participate

Not applicable

Consent for publication

Not applicable

Availability of data and materials

All data generated or analyzed during this study are included in this published article.

Competing interests

The authors declare that they have no competing interests.

Funding

This study was supported by National Innovation Experiment Program for University Students (S202111415127, X202111415207).

Authors' contributions

Qi Lu: Formal analysis, Investigation, Data curation, Writing - original draft, Visualization. Siyi Huang: Formal analysis, Validation. Xiaorui Ma: resources, Investigation.

Acknowledgements

This study was supported by National Innovation Experiment Program for University Students (S202111415127, X202111415207). We thank Prof. Jiawei Chen and Dr. Fanqi Jing from School of Earth Sciences and Resources in China University of Geosciences (Beijing) for data analysis and manuscript polishing.

References

1. Ahmad M., Rajapaksha A.U., Lim J.E., Zhang M., Bolan N., Mohan D., Vithanage M., Lee S.S., Ok Y.S (2014) Biochar as a sorbent for contaminant management in soil and water: a review. Chemosphere 99: 19-33. https://doi.org/10.1016/j.chemosphere.2013.10.071
2. Awual M.R, Ismael M, Khaleque M.A, Yaita T (2014) Ultra-trace copper (II) detection and removal from wastewater using novel meso-adsorbent. J. Ind. Eng. Chem. 20:2332-2340. https://doi.org/10.1016/j.jiec.2013.10.009
3. Barbier F, Duc G, Petit Rame M (2000) Adsorption of lead and cadmium ions from aqueous solution to the montmorillonite/water interface. Colloids and Surfaces A: Physicochem, Eng. Aspects. 166:153-159. https://doi.org/10.1016/S0927-7757(99)00501-4
4. Bi Y, Li R, Guo F, et al (2021) Photocatalytic purification of vehicle exhaust using CeO2–Bi2O3 loaded on white carbon and tourmaline[J]. Environ Sci Pollut Res (5):1-15. https://doi.org/10.1007/ s11356-020-11899-2
5. Cheng W, Wang S.G, Lu L, Gong W.X et al (2008) Removal of malachite green (MG) from aqueous solutions by native and heat-treated anaerobic granular sludge. Biochem. Eng. J. 39:538–

546. https://doi.org/10.1016/j.bej.2007.10.016

6. Chen K.R, Gai X.H, Zhou G.J, Shan Y (2019) Study on a new type of pyroelectric materials with structure of tourmaline. Ceram. Int. 45:10684-10690. https://doi.org/10.1016/j.ceramint.2019.02.139
7. Chen Y, Wang S, Li Y, Liu Y et al (2020) Adsorption of Pb (II) by tourmaline-montmorillonite composite in aqueous phase[J]. J. Colloid Interface Sci. 575:367-376. https://doi.org/10.1016/j.jcis. 2020. 04.110
8. Dinesh, Mohan, Ankur, Pittman, C. U. (2014) Organic and inorganic contaminants removal from water with biochar, a renewable, low cost and sustainable adsorbent – A critical review[J]. Bioresour. Technol. 160:191-202. https://doi.org/10.1016/j.biortech.2014.01.120
9. Duan W.Z, Wang N.F, Xiao W.L, Zhao Y.F et al (2018) Ciprofloxacin adsorption onto different micro-structured tourmaline, halloysite and biotite. J. Mol. Liq. 269: 874-881. https://doi.org/10.1016/j.molliq.2018.08.051
10. Fang Y, Wen J, Zhang H, Wang Q, Hu X (2020) Enhancing Cr (VI) reduction and immobilization by magnetic core-shell structured NZVI@MOF derivative hybrids. Environ. Pollution. 260: 1-9. https://doi.org/10.1016/j.envpol.2020.114021
11. Han Y, Cao X, Ouyang X, Sohi et al (2016) Adsorption kinetics of magnetic biochar derived from peanut hull on removal of Cr (VI) from aqueous solution: Effects of production conditions and particle size[J]. Chemosphere. 145(FEB.):336-41. https://doi.org/10.1016/j.chemosphere.2015.11.050
12. Hawthorne F C, Henry D J (1999) Classification of the minerals of the tourmaline group[J]. Euro J Mineral. 11:201-215. https://doi.org/10.1127/ejm/11/2/0201
13. Jiang X.L, Peng C.J, Fu D, Chen Z et al (2015) Removal of arsenate by ferrihydrite via surface complexation and surface precipitation. Appl. Surf. Sci. (353) 1087-1094. https://doi.org/10.1016/j.apsusc.2015.06.190
14. Jia, Weili, Wang, Cuiping et al (2018) Element uptake and physiological responses of Lactuca sativa upon co-exposures to tourmaline and dissolved humic acids[J]. Environ Sci Pollut Res. 25(16):15998-16008. https://doi.org/10.1007/s11356-018-1751-6
15. Lalhmunsiama S.M, Lee D, Tiwari (2013) Manganese oxide immobilized activated carbons in the remediation of aqueous wastes contaminated with copper (II) and lead (II). Chem. Eng. J. 225:128-137. https://doi.org/10.1016/j.cej.2013.03.083
16. Lehmann J, Gaunt J, Rondon M (2006) Bio-char Sequestration in Terrestrial Ecosystems – A Review. Mitigation and Adaptation Strategies for Global Change. 11(2), 395-419.
17. Le P H, Van H T, Lan H N, Mac D H et al (2019) Removal of Cr (VI) from aqueous solution using magnetic modified biochar derived from raw corncob[J]. New J. Chem. 43(47):1-9. https://doi.org/10.1039/C9NJ02661D
18. Liang N, Ding H, Zha Y P (2010) Preparation and Characterization of Tourmaline/TiO_2 Composite Particles Material[J]. Adv Mat Res. 96:145-150.

https://doi.org/10.4028/www.scientific.net/AMR.96.145

19. Li G.T, Chen D, Zhao W.G, Zhang X.W (2015) Efficient adsorption behavior of phosphate on La-modified tourmaline. J. Environ. Chem. Eng. 3:515-522. https://doi.org/10.1016/ j.jece.2015. .2015.01.010
20. Li Nan, Li Xin, Wang Cuiping (2016) Desorption of Cd (II) from tourmaline at acidic conditions: kinetics, equilibrium and thermodynamics. J. Environ. Chem. Eng. 4:30-36. https://doi.org/10.1016/j.jece.2015.10.015
21. Liu Z.G, Zhang F.S (2011) Removal of copper (II) and phenol from aqueous solution using porous carbons derived from hydrothermal chars. Desalination. 267:101–106. https://doi.org/10.1016/j. desal.2010.09.013
22. Matthew Essandoh, Daniel Womuth, Charles U, Pittman Jr et al (2017) Adsorption of metribuzin from aqueous solution using magnetic and nonmagnetic sustainable low-cost biochar adsorbents. Environ Sci Pollut Res 24:4577-4590. https://doi.org/10.1007/s11356-016-8188-6
23. Mohan D, Sarswat A, Yong S O, Pittman C U (2014) Organic and inorganic contaminants removal from water with biochar, are renewable, low cost and sustainable adsorbent-a critical review. Bioresour. Technol. 160: 191-202. https://doi.org/10.1016/j.biortech.2014.01.120
24. Mostafa, R, Abu Khadra, Belal, Mohamed et al (2019) Facile conversion of kaolinite into clay nanotubes (KNTs) of enhanced adsorption properties for toxic heavy metals (Zn^{2+}, Cd^{2+}, Pb^{2+}, and Cr^{6+}) from water. J. Hazard Mater. 374:296-308. https://doi.org/10.1016/j.jhazmat.2019.04.047
25. Nakamura T., Kubo T (1992) The tourmaline group crystals reaction with water. Ferroelectrics 137, 13–31.
26. Pavithra K.G, Kumar P.S, Christopher F.C, Saravanan. A (2017) Removal of toxic Cr (VI) ions from tannery industrial wastewater using a newly designed three-phase three-dimensional electrode reactor. J. Phys. Chem. Solid. 110:379-38. https://doi.org/10.1016/j.jpcs.2017.07.002
27. Rahman M L, Fui C J, Sarjadi M S, SE Arshad et al (2020) Poly(amidoxime) ligand derived from waste palm fiber for the removal of heavy metals from electroplating wastewater[J]. Environ Sci Pollut Res 27(4): 34541–34556. https://doi.org/10.1007/s11356-020-09462-0
28. Ruan D, Zhang L.N, Zhang Z.J, Xia X.M (2003) Structure and properties of regenerated cellulose/tourmaline nanocrystal composite films. J. Polym. Sci. 42:367-373. https://doi.org/ 10.1002/polb.10664
29. Sobhanardakani S, Parvizimosaed H, Olyaie E (2013) Heavy metals removal from wastewaters using organic solid waste—rice husk[J]. Environ Sci Pollut Res 20:5265-5271. https://doi.org/10.1007/s11356-013-1516-1
30. Wang C.P, Liu J.T, Zhang Zh. Y, Wang BL et al (2012) Adsorption of Cd (II), Ni (II), and Zn (II) by Tourmaline at Acidic Conditions: Kinetics, Thermodynamics, and Mechanisms. Ind. Eng. Chem. Res. 51: 4397-4406. https://doi.org/10.1021/ie2023096
31. Wang C.P, Wu J.Z, Sun H.W, Wang T (2011) Adsorption of Pb (II) ion from aqueous solutions by tourmaline as a novel adsorbent. Ind. Eng. Chem. Res. 50:8515-8523. https://doi.org/10.1021/

ie102520w

32. Wang D, Xu H. D, Ma J, Lu X.H (2018) Strong promoted catalytic ozonation of atrazine at low temperature using tourmaline as catalyst: Influencing factors, reaction mechanisms and pathways. Chem. Eng. J. 354: 113-125. https://doi.org/10.1016/j.cej.2018.07.032
33. Wang F, Meng J.P, Liang J.S, Fang B.Z, Zhang H.C (2019) Insight into the thermal behavior of tourmaline mineral. JOM. 71: 2468-2474. https://doi.org/10.1007/s11837-019-03391-1
34. Wang F, Zhang X.F, Liang J.S, Fang B.Z (2018) Phase transformation and microstructural evolution of black tourmaline mineral powders during heating and cooling processes. Ceram. Int. 44 :13253-13258. https://doi.org/10.1016/j.ceramint.2018.04.154
35. Xia M.S, Hu CH, Zhang H.M (2006) Effects of tourmaline addition on the dehydrogenase activity of Rhodopseudomonas palustri. Process Biochem. 41:221-225. https://doi.org/10.1016/j.procbio.2005.05.012
36. Xu H.Y, Zhao H, Cao N.P, Liu Q, Qi S.Y (2016) Heterogeneous Fenton-like discoloration of organic dyes catalyzed by porous schorl ceramisite. Water Sci. Technol. 74(10):2417-2426. https: //doi.org/10.2166/wst.2016.427
37. Yang S.T, Zhao D.L, Zhang H, Lu S.S et al (2010) Impact of environmental conditions on the sorption behavior of Pb (II) in Na-bentonite suspensions. J. Hazard Mater. 183: 632-640. https://doi.org/
38. YanYang, YuhaoZhang, GuiyinWang, Zhanbiao Yang et al (2021) Adsorption and reduction of Cr (VI) by a novel nanoscale FeS/chitosan/biochar composite from aqueous solution. J. Environ. Chem. Eng. 9 (4): 1-10. https://doi.org/10.1016/j.jece.2021.105407
39. Yao Y.J, Miao S.D, Liu S.Z, Ma L.P et al (2012) Synthesis, characterization, and adsorption properties of magnetic Fe_3O_4/graphene nanocomposite. Chem. Eng. J. 184:326-332. https://doi.org/ 10.1016/j.cej.2011.12.017
40. Yin D.Y, Xu Z.W, Shi J, Shen L.L, He Z.X (2018) Adsorption characteristics of ciprofloxacin on the schorl: kinetics, thermodynamics, effect of metal ion and mechanisms. J. Water. Reuse. Desal. 8:350-359. https://doi.org/10.2166/wrd.2017.143
41. Yu B, Zhang Y, Shukla A, Shukla S.S, Dorris K.L (2000) The removal of heavy metal from aqueous solutions by sawdust adsorption—removal of copper. J Hazard Mater. B 80: 33-42. https://doi.org /10.1016/S0304-3894(00)00278-8
42. Zhang S, Li A, Cui D, Duan S.Y et al (2011) Biological improvement on combined mycelial pellet for aniline treatment by tourmaline in SBR process. Bioresour. Technol. 102:9282-9285. https:// doi.org/10.1016/j.biortech.2011.06.075
43. Zheng Y.Q, Cheng B, You W, Yu J.G (2019) 3D hierarchical graphene oxide-Ni Fe LDH composite with enhanced adsorption affinity to Congo red, methyl orange and Cr (VI) ions. J. Hazard Mater. 369: 214-225. https://doi.org/10.1016/j.jhazmat.2019.02.013
44. Zhou D.H, Kim D.G, S.O. Ko (2015) Heavy metal adsorption with biogenic manganese oxides generated by pseudomonas putida strain MnB1. J. Ind. Eng. Chem. 24:132–139. https:// doi.org/ 10.1016/j.jiec.2014.09.020

45. Zhu D, Liang J, Ding Y, et al (2010) Application of far infrared rare earth mineral composite materials to liquefied petroleum gas [J]. Journal of Nanoscience & Nanotechnology. 10(3):1676. https://doi.org/10.1166/jnn.2010.2070

Figures

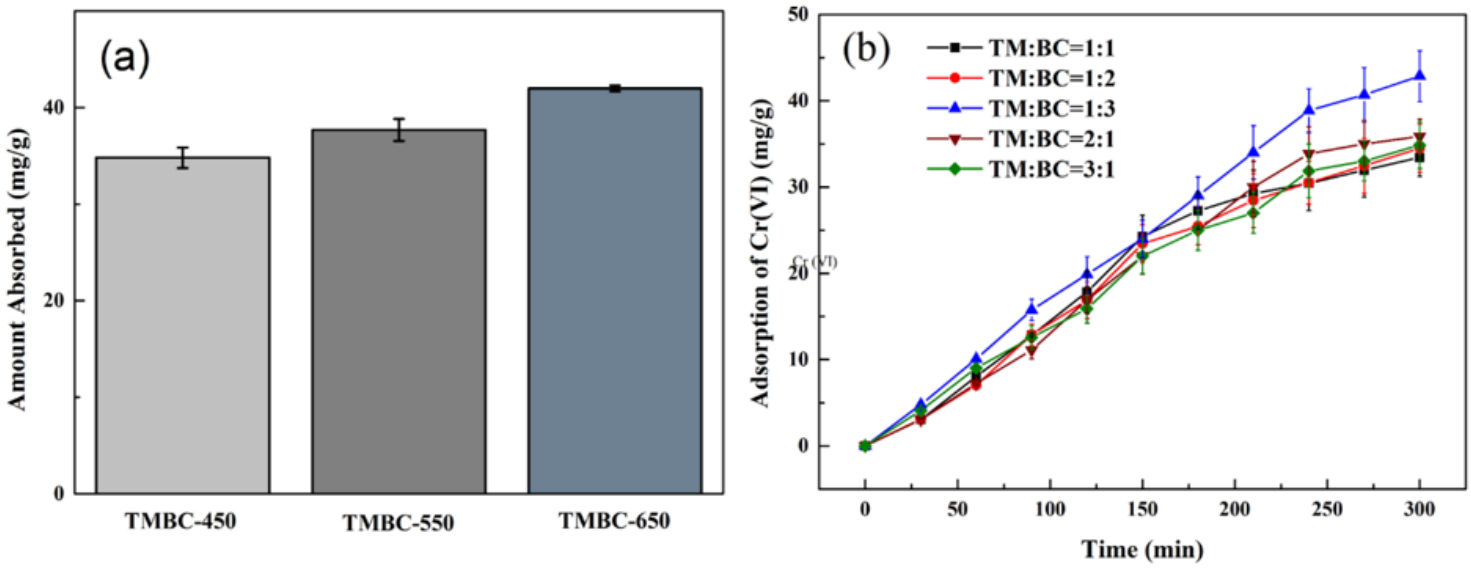

Figure 1

The adsorption of Cr (VI) by (a) different temperature TMBC and (b) different proportions of TMBC-650.

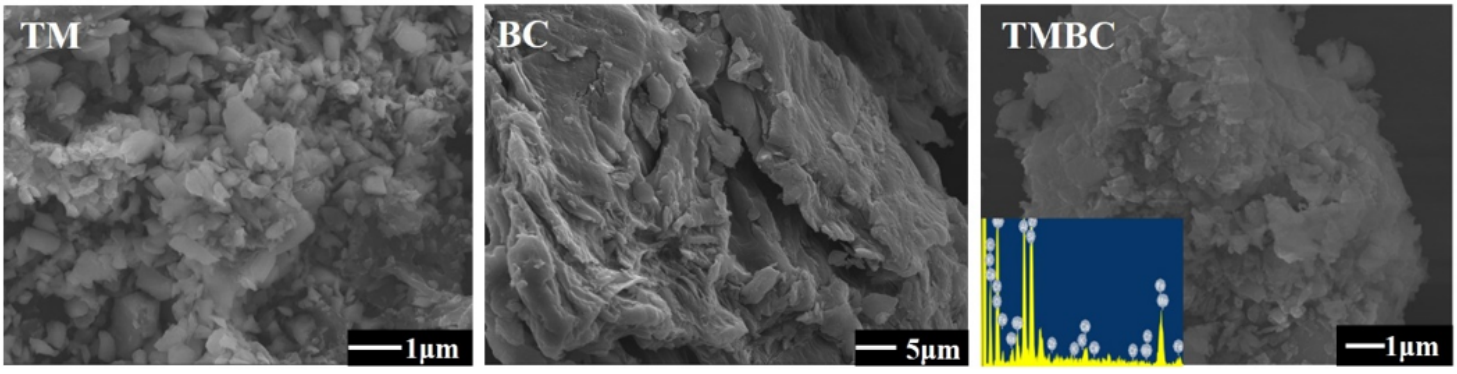

Figure 2

SEM image of (a) tourmaline (TM), (b) biochar (BC), and (c) composite (TMBC).

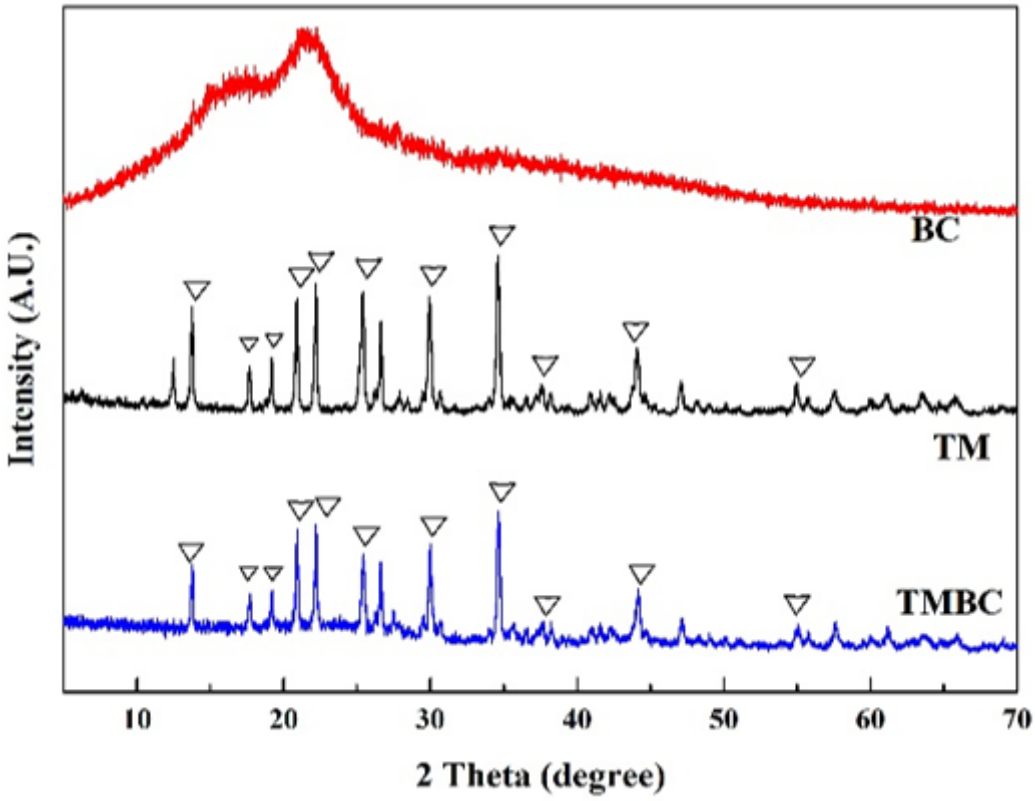

Figure 3

X-ray diffraction patterns of TM, BC and TMBC.

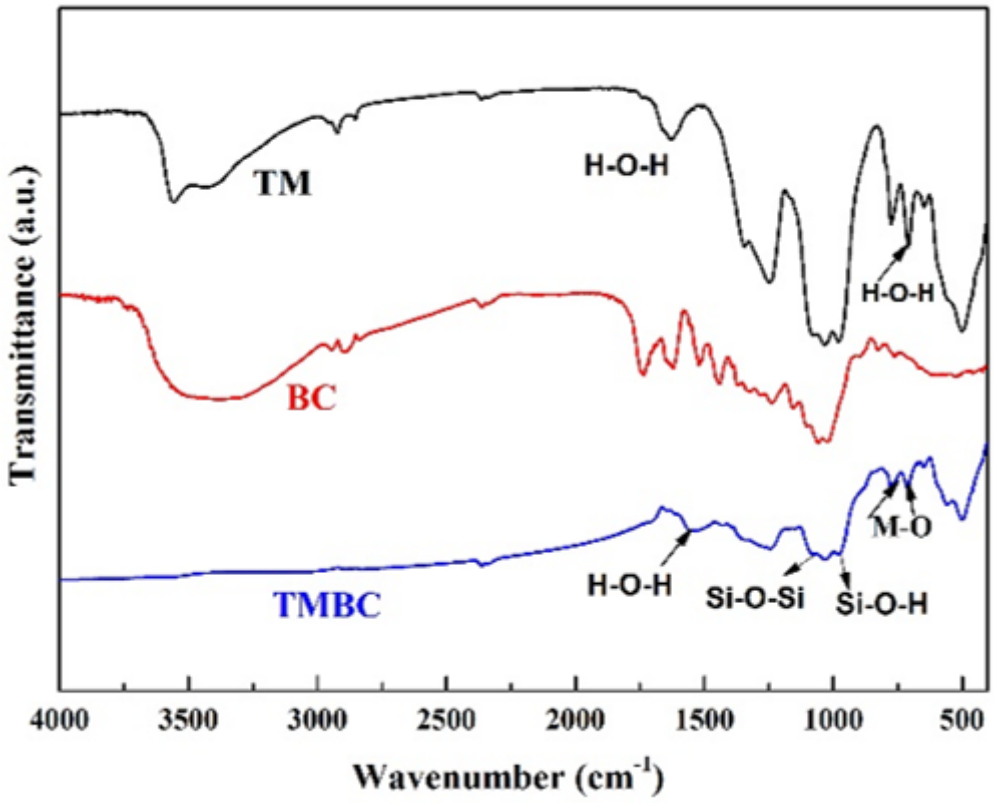

Figure 4

FTIR spectra of TM, BC and TMBC.

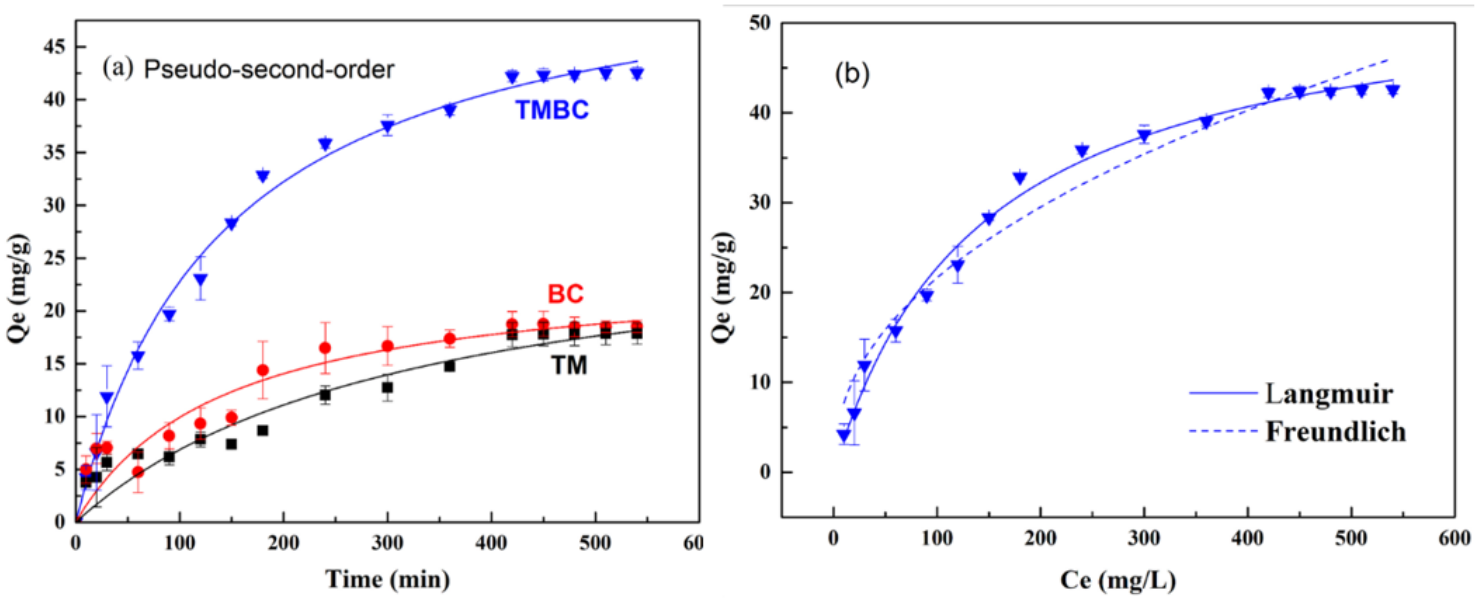

Figure 5

(a) Adsorption kinetics of Cr (VI) by TM, BC, TMBC and (b) adsorption isotherms of TMBC.

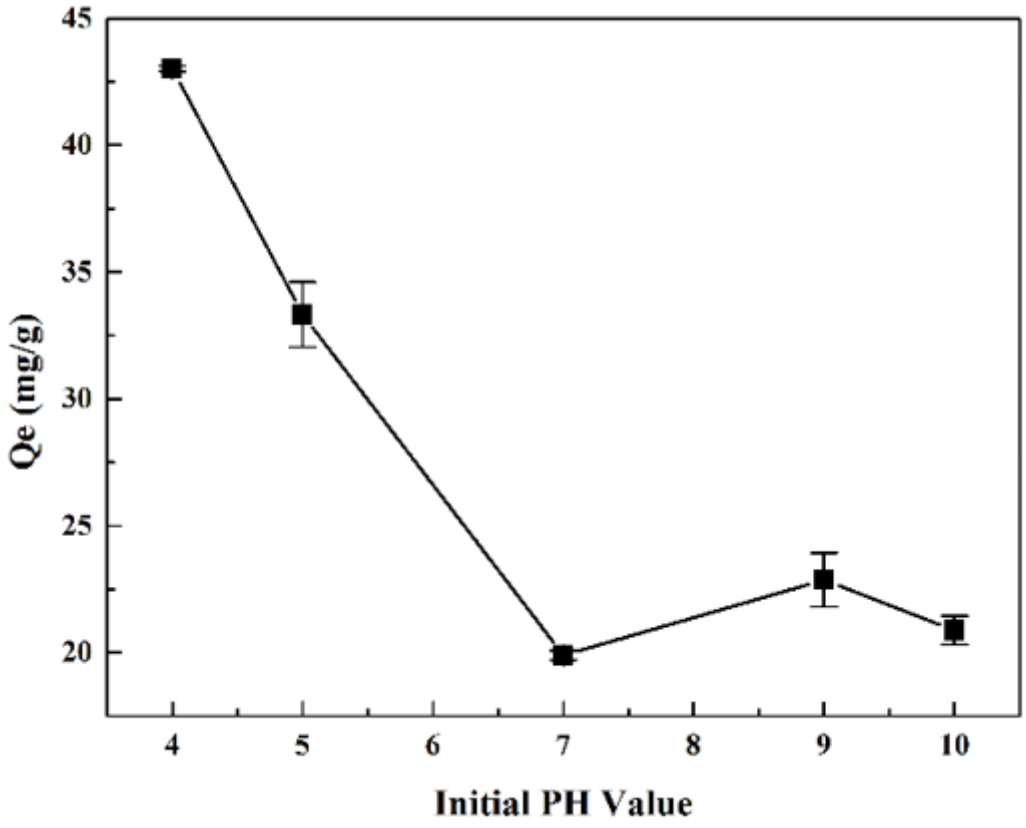

Figure 6

The effect of water pH on Cr (VI) adsorption by TMBC.

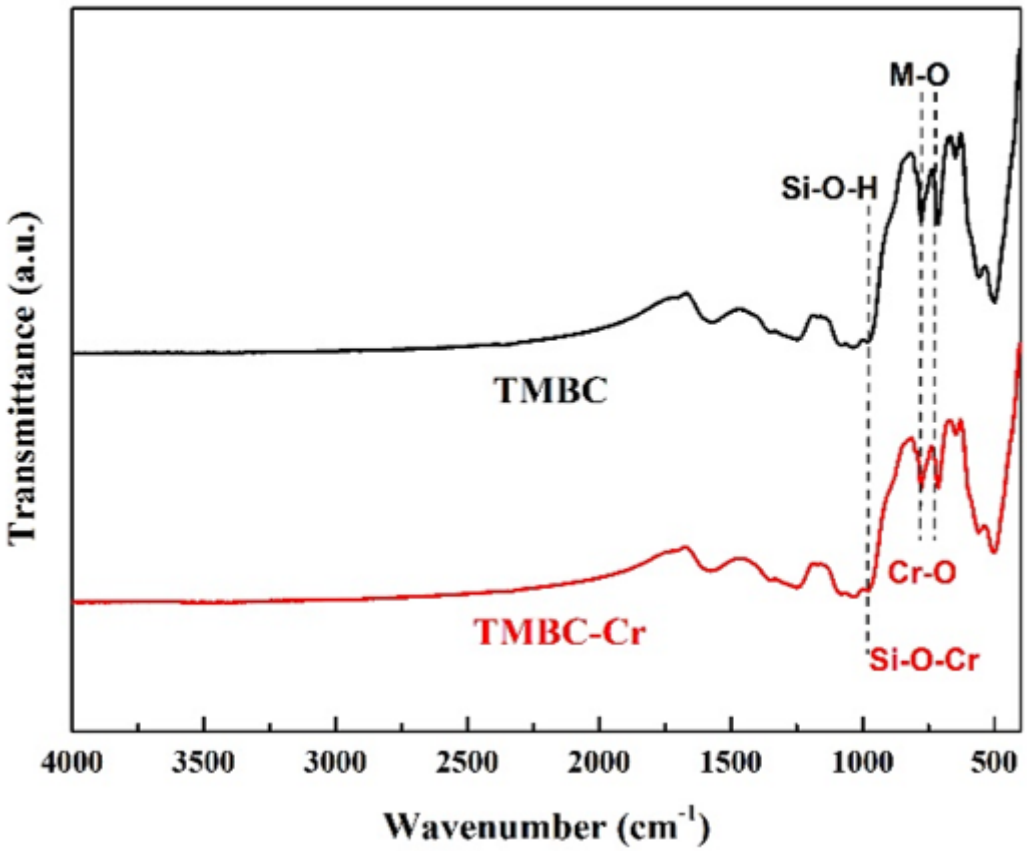

Figure 7

FTIR spectrum of TMBC before and after adsorption of Cr (VI).